Journal of Organometallic Chemistry, 453 (1993) 133–138

JOM 23422

Structural characterization of $[Ru_3(CO)_{10}\{\mu_1\text{-}\eta^2\text{-}cis\text{-}1,2\text{-bis(diphenylphosphino)ethene}\}]$

Kom-Bei Shiu
Department of Chemistry, National Cheng Kung University, Tainan 70101 (Taiwan)

Shie-Ming Peng and Ming-Chu Cheng
Department of Chemistry, National Taiwan University, Taipei 10764 (Taiwan)

(Received September 25, 1992; in revised form November 28, 1992)

Abstract

The structure of $[Ru_3(CO)_{10}(\mu_1\text{-}\eta^2\text{-}c\text{-dpp})]$ (*c*-dpp = *cis*-1,2-bis(diphenylphosphino)ethene) has been determined by X-ray crystallography. The crystals are monoclinic, space group $P2_1/n$, with cell dimensions: $a = 10.4590(17)$, $b = 24.197(6)$, $c = 14.500(4)$ Å, $\beta = 100.003\ (22)°$ and $Z = 4$. This structure was refined to give $R = 0.031$ and $R_w = 0.028$ using 5052 reflections with $I > 2\sigma(I)$ in the range of $2 \leq 2\theta \leq 50°$ (Mo $K\alpha$). The structure suggested previously to contain a 1,2-bridging *c*-dpp ligand is now found to contain the ligand in a 1,1-chelating geometry, which is also maintained in solution as indicated by the large downfield ^{31}P coordination shift. This five-membered chelate ring is not perpendicular as observed for a similar ring in $[Ru_3(CO)_{10}(\mu_1\text{-}\eta^2\text{-bipy})]$ (bipy = 2,2′-bipyridine) but nearly coplanar with the Ru_3 plane. The synthesis and the structures of $[M_3(CO)_{10}(L\text{–}L)]$ and $[M_2(CO)_6(L\text{–}L)]$ (M = Fe, Ru or Os; L–L = chelating *c*-dpp or bridging 1,2-bis(dimethylarsino)tetrafluorocyclobutene) are compared and a general reaction mechanism from $[M_3(CO)_{12}]$ to $[M_3(CO)_{10}(L\text{–}L)]$ and $[M_2(CO)_6(L\text{–}L)]$ is proposed.

1. Introduction

Following the discovery of the intramolecular η^2-arene compound, $[Mo(PhHCPz'2)(CO)_3]$ (Pz′ = 3,5-dimethylpyrazol-1-yl) [1], we became interested in the bidentate ligand containing an olefinic chain between two donor atoms and the relevant metal carbonyl derivatives [2]. In this paper, we wish to present the accidental discovery that the structure of $[Ru_3(CO)_{10}(c\text{-dpp})]$ includes a chelating phosphorus-bidentate ligand, *cis*-1,2-bis(diphenylphosphino)ethene (*c*-dpp), rather than a bridging *c*-dpp as suggested previously [3].

Ligands such as *c*-dpp or 1,2-bis(dimethylarsino)-tetrafluorocyclobutene (dma) and their derivatives $[Ru_3\text{-}(CO)_{10}(c\text{-dpp})]$ (**1**), $[Ru_2(CO)_6(c\text{-dpp})]$ (**2**) [3], $[Ru_3\text{-}(CO)_{10}(dma)]$ (**3**), $[Ru_2(CO)_6(dma)]$ (**4**) [4], $Fe_3\text{-}(CO)_{10}(dma)]$ (**5**), and $[Fe_2(CO)_6(dma)]$ (**6**) [5] have been described. It is apparent from the synthetic procedures reported that all these derivatives of the ligands were formed by a similar pathway from $[M_3(CO)_{12}]$ (M = Fe or Ru), first forming $[M_3(CO)_{10}(L\text{–}L)]$ (L–L = *c*-dpp or dma) and then $[M_2(CO)_6(L\text{–}L)]$ [3,4a,5c]. The $\nu(CO)$ patterns of **1**, **3** and $[Ru_3(CO)_{10}(\mu\text{-dppe})]$ (**7**) (dppe = 1,2-bis(diphenylphosphino)ethane) [6] are quite similar to each other and the structure of **3** [4c] was also found to be similar to that of **7** [6b]. Coincidentally, the similarity in the $\nu(CO)$ patterns of **2**, **4** and **6** also parallels that in the structures of **2** [3] and **6** [5a]. The structure of **1** is therefore proposed to be like that of **6**; *i.e.*, $[Ru_3(CO)_{10}(\mu\text{-}c\text{-dpp})]$ with a bridging *c*-dpp ligand [3].

However, there are quite a few instances in the literature where the coordination mode was erroneously assigned before the final confirmation by X-ray crystallography. For examples, dppe in $[Ru_3(CO)_{10}(dppe)]$ was suggested to be chelating in 1972 [6a] but found to be bridging in 1982 [6b] and 2,2′-bipyridine (bipy) in $[Ru_3(CO)_{10}(bipy)]$ (**8**) was also first proposed as bridging [7] but later confirmed as chelating [8]. Whether the substitution geometry is 1,1-chelating or

---

Correspondence to: Dr. K.-B. Shiu.

0022-328X/93/$6.00

1,2-bridging depends on a variety of factors, such as the chain length [9] or steric bulk [10] between the two ligating atoms of the bidentate ligands. Interconversions between these two and further modes are also known [9a,b,11], probably due to relative stabilities [12]. Obviously, it is not a question of a simple connection between the structure and the IR spectral data. Besides, some carbonyl stretching bands of weak intensity, which are informative, are usually overlooked [7,8].

Since it has been noted several times [11c,13] that a phosphorus atom involved in a five-membered chelate ring experiences anomalously large nuclear deshielding upon coordination and exhibits a small downfield coordination shift in a six-membered ring, we decided to measure $^{31}P\{^1H\}$ NMR for **1** and the free *c*-dpp ligand. As shown below, the measurements then led us to suspect that the *c*-dpp coordination in this compound should not be bridging but chelating, although both the chelating and the bridging *c*-dpp ligands had been observed previously [9c,12]. In order to confirm the assignment and compare the orientations of the five-membered chelate rings with respect to the metal skeleton in this and other structures (metal-cluster compounds containing a chelating bidentate have only rarely been characterized by X-ray crystallography [8,11b]), the crystal structure of **1** was studied and related features are reported here.

2. Experimental section

Compound **1** was obtained by the published procedure [3]. The IR spectrum of **1** in cyclohexane was measured using a Bio-Rad Digilab 3260 FT-IR spectrometer: ν(CO), 2084m, 2063w, 2034s, 2015m, 2005vs, 1992w, 1980w, 1970m, and 1940w cm^{-1}. $^{31}P\{^1H\}$ NMR spectra of *c*-dpp and **1** dissolved in acetone-d_6 were obtained at 296 K by a Bruker AMX-400 FT NMR spectrometer at 162 MHz in 5 mm stationary tubes with a 2 mm reference tube (the Wilmad special stem insert) of 85% H_3PO_4: −21.6 and 69.6 ppm, respectively. ^1H NMR (acetone-d_6, 296 K, 400 MHz): C_2H_2, δ 8.20 (m, 1H), 8.08 (m, 1H); Ph, 7.52 (m, 10H), 7.50 (m, 10H). Elementary analysis results (Found: C, 44.18; H, 2.33; $C_{36}H_{22}O_{10}P_2Ru_3$ calcd.: C, 44.13; H, 2.26%) were obtained by the staff of the microanalytical Service of the Department of Chemistry, National Cheng Kung University.

Red crystals of **1**, suitable for X-ray diffraction studies, were grown from CH_2Cl_2/hexane at room temperature. They are monoclinic and belong to the space group $P2_1/n$, and refined cell constants and other crystallographic information are summarized in Table 1. The methods used have been presented elsewhere [14]. All non-hydrogen atoms were refined anisotropically. The final refinement converged smoothly and no chemically significant peaks were found in the final difference map.

TABLE 1. Crystal data for [$Ru_3(CO)_{10}(\mu_1$-η^2-(c-dpp))] (**1**)

Empirical formula	$C_{36}H_{22}O_{10}P_2Ru_3$
Color	red
Crystal size (mm)	0.40 × 0.40 × 0.50 mm
Space group	monoclinic, $P2_1/n$
Unit cell dimensions	a = 10.4590(17) Å b = 24.197(6) Å c = 14.500(4) Å β = 100.003(22)°
Volume	3613.8(15) Å^3
Z	4
Formula weight	979.72
Density (calc.)	1.801 g cm^{-3}
Orientatn. rflns., 2θ range	24, 18.84–23.42°
h, k, l ranges	−12 to 12, 0 to 28, 0 to 17
Absorption correction	ψ scan
Abs coeff.	1.36 mm^{-1}
Transm. range	0.8637–0.9997
$F(000)$	1919.79
Diffractometer used	Nonius CAD4
Radiation	Mo Kα (λ = 0.70930 Å)
Temperature	297 K
2θ range	2–50°
Scan type	$\theta/2\theta$
Scan speed	variable, 2.06–8.24° min^{-1}
Scan param.	1.6 + 0.7 tan θ
Std. rflns. (No. 3)	variations < 2%, 2σ; every 7200 sec
No. of unique data	6358
No. of data (N_o) with $I > 2.0\sigma(I)$	5052
No. of atoms and params (N_v) refined	73, 461
Max Δ/σ ratio	0.406
R; [a] R_w [b]	0.031; 0.028
GOF [c]	2.87
Max/min resid. electron density	0.57/−0.56 e Å^{-3}

[a] $R = \Sigma||F_o| - |F_c||/\Sigma|F_o|$.
[b] $R_w = [\Sigma w(|F_o| - |F_c|)^2/\Sigma w|F_o|]^{1/2}$.
[c] $w = 1/\sigma^2(F_o)$; GOF $= [\Sigma w(|F_o| - |F_c|)^2/(N_o - N_v)]^{1/2}$.

The fractional atomic coordinates of all the non-hydrogen atoms are listed in Table 2. Table 3 contains selected bond lengths and angles. Tables of fractional atomic coordinates of the hydrogen atoms and the anisotropic temperature factors of all other atoms, and the listing of structure factor (F_o *vs.* F_c) are available from the authors. The ORTEP plot of **1** with the numbering scheme is shown in Fig. 1.

3. Results and discussion

As shown in Fig. 1, the *c*-dpp ligand is found as a chelating bidentate with two phosphorus atoms, P(1) and P(2), connected with Ru(1). This five-membered chelate-ring structure is also maintained in solution as shown by the large ^{31}P downfield coordination shift of 91.2 ppm observed for **1**. Although the variable-temperature NMR studies have been known to give the correct assignment of coordination mode in $[Ru_3(CO)_{10}(\mu\text{-dppm})]$ (**9**) (dppm = 1,2-bis(diphenylphosphino)methane) [15], it is rather time-consuming. Thus, we wish to re-emphasize here the importance of ^{31}P NMR as a simple but sensitive probe to complete the task.

TABLE 2. Fractional atomic coordinates and B_{iso} for **1**

Atom	*x*	*y*	*z*	B_{iso} [a]
Ru1	0.25674(4)	0.325467(12)	0.239685(25)	2.318(14)
Ru2	0.29259(4)	0.220332(15)	0.15021(3)	3.306(19)
Ru3	0.21356(4)	0.221543(15)	0.32967(3)	3.436(19)
P1	0.31432(11)	0.39472(5)	0.14676(8)	2.78(5)
P2	0.20192(12)	0.39567(5)	0.33226(8)	2.85(5)
C1	0.2807(5)	0.46012(17)	0.1992(3)	3.59(23)
C2	0.2357(5)	0.46050(17)	0.2782(3)	3.78(25)
C3	0.0865(4)	0.32423(18)	0.1640(3)	2.90(19)
O3	−0.0137(3)	0.32807(14)	0.11901(21)	4.20(17)
C4	0.4276(4)	0.32310(18)	0.3143(3)	2.89(20)
O4	0.5289(3)	0.32614(14)	0.35803(22)	4.41(17)
C5	0.1092(5)	0.21516(19)	0.1002(3)	3.9(3)
O5	0.0044(4)	0.20861(14)	0.06386(22)	5.20(19)
C6	0.4731(5)	0.22824(20)	0.2062(3)	4.3(3)
O6	0.5833(4)	0.22906(16)	0.23118(24)	5.88(21)
C7	0.3123(6)	0.14265(21)	0.1425(3)	4.9(3)
O7	0.3278(4)	0.09655(15)	0.1368(3)	7.6(3)
C8	0.3267(5)	0.24564(22)	0.0322(3)	4.6(3)
O8	0.3466(4)	0.25786(17)	−0.03924(24)	7.0(3)
C9	0.0332(5)	0.23005(21)	0.2727(3)	4.5(3)
O9	−0.0761(4)	0.23165(17)	0.24744(25)	6.14(22)
C10	0.3968(5)	0.21515(19)	0.3800(3)	4.1(3)
O10	0.5016(4)	0.20762(14)	0.41550(23)	5.36(19)
C11	0.1898(6)	0.14374(21)	0.3418(3)	5.2(3)
O11	0.1744(5)	0.09847(15)	0.3493(3)	8.5(3)
C12	0.1812(5)	0.25010(22)	0.4463(3)	4.8(3)
O12	0.1603(4)	0.26370(17)	0.51703(24)	7.2(3)
C11A	0.2254(4)	0.40381(19)	0.0272(3)	3.55(21)
C12A	0.1037(5)	0.42799(22)	0.0120(4)	5.1(3)
C13A	0.0359(6)	0.4342(3)	−0.0796(5)	7.6(4)
C14A	0.0900(8)	0.4158(3)	−0.1524(4)	8.9(4)
C15A	0.2095(7)	0.3911(3)	−0.1375(4)	8.3(4)
C16A	0.2759(6)	0.38542(24)	−0.0493(3)	5.3(3)
C11B	0.4823(4)	0.40437(19)	0.1306(3)	3.59(22)
C12B	0.5317(6)	0.45553(24)	0.1150(6)	8.5(5)
C13B	0.6587(7)	0.4602(3)	0.1006(6)	10.2(5)
C14B	0.7374(5)	0.4167(3)	0.1010(5)	6.5(4)
C15B	0.6901(5)	0.36687(23)	0.1157(4)	5.2(3)
C16B	0.5631(5)	0.36042(20)	0.1300(3)	4.2(3)
C21A	0.0351(5)	0.40707(20)	0.3492(3)	3.77(23)
C22A	−0.0507(5)	0.36464(22)	0.3455(4)	4.6(3)
C23A	−0.1765(5)	0.3720(3)	0.3607(4)	5.9(3)
C24A	−0.2175(6)	0.4219(3)	0.3798(5)	7.6(4)
C25A	−0.1340(7)	0.4647(3)	0.3859(7)	11.5(6)
C26A	−0.0076(6)	0.45818(25)	0.3699(6)	9.3(5)
C21B	0.2939(5)	0.40513(19)	0.4510(3)	3.92(24)
C22B	0.4172(6)	0.42713(22)	0.4630(4)	5.7(3)
C23B	0.4873(7)	0.4340(3)	0.5532(5)	9.0(4)
C24B	0.4362(9)	0.4193(3)	0.6267(5)	11.0(5)
C25B	0.3155(9)	0.3966(3)	0.6176(4)	10.4(5)
C26B	0.2436(6)	0.3902(3)	0.5290(4)	6.2(3)

[a] B_{iso} is the mean of the principal axes of the thermal ellipsoid.

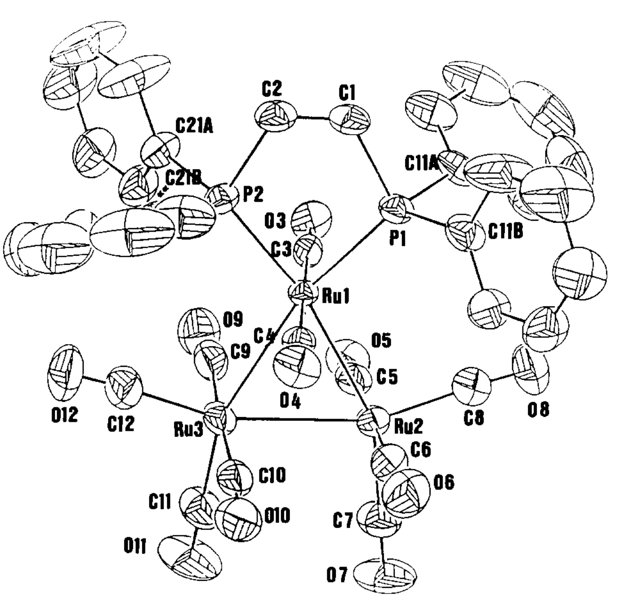

Fig. 1. ORTEP drawing of $[Ru_3(CO)_{10}(\mu_1\text{-}\eta^2\text{-}(c\text{-dpp}))]$ (**1**) with the numbering scheme. Thermal ellipsoids are drawn at the 50% probability level.

In contrast to the structure of **8** containing a chelating bipy perpendicular to the metal skeleton, the five-membered chelate ring plane, defined by P(1), C(1), C(2), P(2), and Ru(1) in **1** is nearly coplanar with the trinuclear Ru_3 plane (the angle formed by these two planes is 5.29(3)°). This different feature influences the two structures quite largely. As the chelating *c*-dpp ligand is coordinated at equatorial sites around Ru(1), it introduces a significant distortion with the significantly shorter Ru(2)–Ru(3) bond length of 2.8641(10) Å compared with those of 2.9094(7) and 2.9043(7) Å (Table 3) for Ru(1)–Ru(2) and Ru(1)–Ru(3) bonds, respectively, into the trinuclear Ru_3 core as compared with $[Ru_3(CO)_{12}]$ [16] (Ru–Ru range 2.851(1)–2.859(1) Å). At the same time it maintains the nearly linear geometry of all carbonyl groups, as observed in **7**, **9**, or $[Ru_3(CO)_{11}(PPh_3)]$ [17]. In **8**, however, two carbonyl groups asymmetrically bridge the shortest Ru–Ru bond, one of two Ru–Ru bonds *cis* to bipy [8]. Why the phosphine ligands prefer equatorial positions rather than axial positions as observed in **8** is not clear at this moment. Since the IR spectrum in the carbonyl region and the ^{31}P NMR spectrum of $[Ru_3(CO)_{10}(dmpm)]$ (dmpm = 1,2-bis(dimethylphosphino)methane) [18] also indicates that the smaller dmpm takes the bridging,

TABLE 3. Selected bond lengths (Å) and bond angles (°)

Ru(1)–Ru(2)	2.9094(7)	C(9)–O(9)	1.139(7)
Ru(1)–Ru(3)	2.9043(7)	C(10)–O(10)	1.142(6)
Ru(1)–P(1)	2.2952(12)	C(11)–O(11)	1.115(6)
Ru(1)–P(2)	2.2985(12)	C(12)–O(12)	1.133(6)
Ru(1)–C(3)	1.922(4)	C(11A)–C(12A)	1.383(7)
Ru(1)–C(4)	1.922(4)	C(11A)–C(16A)	1.381(7)
Ru(2)–Ru(3)	2.8641(10)	C(12A)–C(13A)	1.402(8)
Ru(2)–C(5)	1.933(5)	C(13A)–C(14A)	1.356(11)
Ru(2)–C(6)	1.931(5)	C(14A)–C(15A)	1.368(11)
Ru(2)–C(7)	1.896(5)	C(15A)–C(16A)	1.353(8)
Ru(2)–C(8)	1.908(5)	C(11B)–C(12B)	1.375(7)
Ru(3)–C(9)	1.934(6)	C(11B)–C(16B)	1.359(7)
Ru(3)–C(10)	1.935(5)	C(12B)–C(13B)	1.385(8)
Ru(3)–C(11)	1.911(5)	C(13B)–C(14B)	1.335(9)
Ru(3)–C(12)	1.911(5)	C(14B)–C(15B)	1.335(8)
P(1)–C(1)	1.816(4)	C(15B)–C(16B)	1.388(7)
P(1)–C(11A)	1.833(5)	C(21A)–C(22A)	1.359(7)
P(1)–C(11B)	1.828(5)	C(21A)–C(26A)	1.366(7)
P(2)–C(2)	1.815(4)	C(22A)–C(23A)	1.383(7)
P(2)–C(21A)	1.825(5)	C(23A)–C(24A)	1.328(9)
P(2)–C(21B)	1.835(5)	C(24A)–C(25A)	1.348(10)
C(1)–C(2)	1.312(6)	C(25A)–C(26A)	1.390(9)
C(3)–O(3)	1.138(5)	C(21B)–C(22B)	1.378(8)
C(4)–O(4)	1.138(5)	C(21B)–C(26B)	1.376(7)
C(5)–O(5)	1.142(6)	C(22B)–C(23B)	1.393(8)
C(6)–O(6)	1.147(7)	C(23B)–C(24B)	1.322(12)
C(7)–O(7)	1.132(6)	C(24B)–C(25B)	1.362(13)
C(8)–O(8)	1.131(6)	C(25B)–C(26B)	1.380(9)
Ru(2)–Ru(1)–Ru(3)	59.029(21)	Ru(1)–P(2)–C(2)	107.44(15)
Ru(2)–Ru(1)–P(1)	108.02(4)	Ru(1)–P(2)–C(21A)	122.13(16)
Ru(2)–Ru(1)–P(2)	166.20(3)	Ru(1)–P(2)–C(21B)	119.79(15)
Ru(2)–Ru(1)–C(3)	84.86(13)	C(2)–P(2)–C(21A)	100.94(23)
Ru(2)–Ru(1)–C(4)	92.61(13)	C(2)–P(2)–C(21B)	100.79(22)
Ru(3)–Ru(1)–P(1)	166.66(3)	C(21A)–P(2)–C(21B)	102.26(22)
Ru(3)–Ru(1)–P(2)	107.66(4)	P(1)–C(1)–C(2)	119.8(3)
Ru(3)–Ru(1)–C(3)	92.41(13)	P(2)–C(2)–C(1)	119.8(3)
Ru(3)–Ru(1)–C(4)	85.61(13)	Ru(1)–C(3)–O(3)	174.4(4)
P(1)–Ru(1)–P(2)	85.46(5)	Ru(1)–C(4)–O(4)	174.6(4)
P(1)–Ru(1)–C(3)	89.31(13)	Ru(2)–C(5)–O(5)	173.0(4)
P(1)–Ru(1)–C(4)	92.23(13)	Ru(2)–C(6)–O(6)	172.1(4)
P(2)–Ru(1)–C(3)	92.54(13)	Ru(2)–C(7)–O(7)	177.7(5)
P(2)–Ru(1)–C(4)	89.74(13)	Ru(2)–C(8)–O(8)	176.4(5)
C(3)–Ru(1)–C(4)	177.35(18)	Ru(3)–C(9)–O(9)	172.3(4)
Ru(1)–Ru(2)–Ru(3)	60.396(15)	Ru(3)–C(10)–O(10)	173.3(4)
Ru(1)–Ru(2)–C(5)	91.59(13)	Ru(3)–C(11)–O(11)	179.1(5)
Ru(1)–Ru(2)–C(6)	85.32(14)	Ru(3)–C(12)–O(12)	175.6(5)
Ru(1)–Ru(2)–C(7)	156.47(15)	P(1)–C(11A)–C(12A)	120.2(4)
Ru(1)–Ru(2)–C(8)	100.24(16)	P(1)–C(11A)–C(16A)	121.2(4)
Ru(3)–Ru(2)–C(5)	85.27(13)	C(12A)–C(11A)–C(16A)	118.6(4)
Ru(3)–Ru(2)–C(6)	91.88(13)	C(11A)–C(12A)–C(13A)	119.7(5)
Ru(3)–Ru(2)–C(7)	96.63(15)	C(12A)–C(13A)–C(14A)	119.4(6)
Ru(3)–Ru(2)–C(8)	160.00(16)	C(13A)–C(14A)–C(15A)	121.0(5)
C(5)–Ru(2)–C(6)	176.56(19)	C(14A)–C(15A)–C(16A)	119.9(6)
C(5)–Ru(2)–C(7)	91.40(22)	C(11A)–C(16A)–C(15A)	121.4(6)
C(5)–Ru(2)–C(8)	90.68(21)	P(1)–C(11B)–C(12B)	122.2(4)
C(6)–Ru(2)–C(7)	90.85(22)	P(1)–C(11B)–C(16B)	120.9(3)
C(6)–Ru(2)–C(8)	91.36(21)	C(12B)–C(11B)–C(16B)	116.9(4)
C(7)–Ru(2)–C(8)	103.05(22)	C(11B)–C(12B)–C(13B)	119.7(5)
Ru(1)–Ru(3)–Ru(2)	60.575(15)	C(12B)–C(13B)–C(14B)	122.8(6)
Ru(1)–Ru(3)–C(9)	86.12(14)	C(13B)–C(14B)–C(15B)	117.9(5)
Ru(1)–Ru(3)–C(10)	91.00(13)	C(14B)–C(15B)–C(16B)	121.1(5)

TABLE 3 (continued)

Ru(1)–Ru(3)–C(11)	158.00(15)	C(11B)–C(16B)–C(15B)	121.7(5)
Ru(1)–Ru(3)–C(12)	98.62(16)	P(2)–C(21A)–C(22A)	121.4(4)
Ru(2)–Ru(3)–C(9)	91.57(13)	P(2)–C(21A)–C(26A)	121.6(4)
Ru(2)–Ru(3)–C(10)	85.33(13)	C(22A)–C(21A)–C(26A)	117.0(5)
Ru(2)–Ru(3)–C(11)	97.83(15)	C(21A)–C(22A)–C(23A)	122.5(5)
Ru(2)–Ru(3)–C(12)	158.64(16)	C(22A)–C(23A)–C(24A)	120.1(5)
C(9)–Ru(3)–C(10)	176.54(19)	C(23A)–C(24A)–C(25A)	118.9(5)
C(9)–Ru(3)–C(11)	90.65(23)	C(24A)–C(25A)–C(26A)	121.8(6)
C(9)–Ru(3)–C(12)	91.71(22)	C(21A)–C(26A)–C(25A)	119.7(6)
C(10)–Ru(3)–C(11)	91.30(22)	P(2)–C(21B)–C(22B)	119.6(4)
C(10)–Ru(3)–C(12)	90.63(21)	P(2)–C(21B)–C(26B)	121.7(4)
C(11)–Ru(3)–C(12)	103.23(21)	C(22B)–C(21B)–C(26B)	118.7(5)
Ru(1)–P(1)–C(1)	107.50(15)	C(21B)–C(22B)–C(23B)	119.6(6)
Ru(1)–P(1)–C(11A)	120.08(15)	C(22B)–C(23B)–C(24B)	120.3(7)
Ru(1)–P(1)–C(11B)	121.66(15)	C(23B)–C(24B)–C(25B)	121.9(6)
C(1)–P(1)–C(11A)	100.86(22)	C(24B)–C(25B)–C(26B)	118.8(6)
C(1)–P(1)–C(11B)	101.71(22)	C(21B)–C(26B)–C(25B)	120.8(6)
C(11A)–P(1)–C(11B)	101.78(21)		

equatorial positions, it is probably true that electronic factors are more important than steric in determining the preferred coordination positions.

There is an approximate C_2 axis in **1** through the Ru(1) atom and the mid-points of the Ru(2)–Ru(3) and the C(1)–C(2) bonds (Ru(1)–P(1) = 2.2952(12) *vs.* Ru(1)–P(2) = 2.2985(12); P(1)–C(1) = 1.816(4) *vs.* P(2)–C(2) = 1.815(4); Ru(2)–C(5) = 1.933(5) *vs.* Ru(3)–C(10) = 1.935(5); Ru(2)–C(6) = 1.931(5) *vs.* Ru(3)–C(9) = 1.934(5) Å). As reflected in the bond angles, Ru(1)–Ru(2)–C(8) = 100.24(16) and Ru(1)–Ru(3)–C(12) = 98.62(16)°, the plane including P(1), P(2), C(1), C(2), and Ru(1) is slightly distorted from the perfect coplanar position with respect to the Ru_3 plane toward the Ru(1)–Ru(2) side, and probably relieves nonbonded interactions between the *c*-dpp phenyl groups and the equatorial CO groups (Fig. 1). As observed previously in $[Ru_3(CO)_8(\mu\text{-dppm})_2]$ [19] and in $[Ru_3(CO)_{10}(\mu\text{-dppm})]$ (**9**) [15b] that the Ru–Ru bonds supported by the bridging phosphine-bidentate ligands are shortened, the average Ru–Ru distance in **1** (2.893 Å) is indeed much longer than that of 2.853 Å in **7** [6b], that of 2.845 Å in **9** [15b] and that of 2.840 Å in **3** [4c] and comparable with that of 2.88 Å in **10** [17]. However, the average Ru–Ru value is 2.854 Å in $[Ru_3(CO)_{12}]$ [16], appreciably shorter than that in **1** or **10**. Since the two metal–metal bonds *cis* to the bulky substituent are longer than the third unique one in these two structures (2.9094(7) and 2.9043(7) *vs.* 2.8641(10) Å in **1** and 2.907(3) and 2.876(3) *vs.* 2.875(3) Å in **10**), the increased metal–metal bond lengths may indicate the steric effect induced by the substituent, which was commented upon earlier in the $P(OMe)_3$ derivative of $[Os_3(CO)_{12}]$ [20].

The C=C bond length of 1.312(6) Å is within the range of 1.30–1.33 Å found for the uncoordinated C=C bond of *c*-dpp in $[Ir_4(CO)_8(\mu\text{-}c\text{-dpp})_2]$ [12]. The average P–C(phenyl) and P–C(ethene) distances (1.830 and 1.816 Å) are likewise unexceptional. The Ru–P distances of 2.2952(12) and 2.2985(12) Å in **1** are shorter than those of 2.366(1) and 2.376(1) Å in **2** [3]. Since the bonding interaction between the C=C bond of *c*-dpp in this compound seems quite strong, as evidenced by the C–C distance of 1.445(5) Å in **2**, that of 1.435(16) Å in $[Ir_3(CO)_7(\mu\text{-}(cis\text{-}(PPhCH{=}CHPPh_2)))]$ [21], and those of the uncoordinated C=C bonds in **1** and $[Ir_4(CO)_8(\mu\text{-}$

$$\begin{tikzcd}
{[M_3(CO)_{12}]} \arrow[r, "\Delta", "\substack{+L-L\\ -2\,CO}"'] & {[M_3(CO)_{10}(\mu_2\text{-}\eta^2\text{-}(L-L))]} \arrow[d, shift right, "\Delta"'] \\
\text{M = Fe, Ru, or Os} & \\
{[M_2(CO)_6(L-L)]} & {[M_3(CO)_{10}(\mu_1\text{-}\eta^2\text{-}(L-L))]} \arrow[l, "\Delta"', "-\text{“M(CO)}_4\text{”}"] \arrow[u, shift right, "\Delta"'] \\
\text{M = Fe or Ru} &
\end{tikzcd}$$

Scheme 1.

c-dpp$)_2$] [12], it is clear that the coordination of the olefinic moiety of *c*-dpp affords considerable stabilization to the structure of **2** so that the conversion from **1** to **2** is feasible with breaking two Ru–Ru bonds to extrude the "$Ru(CO)_4$" unit and at the same time lengthening the two Ru–P distances in **1**. Probably, at high temperatures, **3** and **5** isomerize first to the unknown chelating compound, [$M_3(CO)_{10}(\mu_1$-η^2-dma)], and then form **4** and **6**, respectively, by extruding the "$M(CO)_4$" unit. Thus, as observed in other systems [9a,b,11], the structures containing bridging or chelating *c*-dpp or dma in [$M_3(CO)_{10}$(L–L)] (L–L = *c*-dpp or dma) may have comparable stability and can interconvert to each other in solution at high temperatures. We believe that the subsequent coordination of the olefinic moiety of the chelating *c*-dpp or dma in **1** or the unknown [$M_3(CO)_{10}(\mu_1$-η^2-dma)] complete the conversion from [$M_3(CO)_{12}$] to **2**, **4**, and **6** [3–5]. This conversion pathway may also apply in the osmium analogues and is supported by the fact that the thermolysis of [$Os_3(CO)_{10}$(*c*-dpp)] did not give any product such as [$Os_2(CO)_6$(*c*-dpp)] [3], obviously due to the Os–Os bond being stronger than the Ru–Ru bond [22], whether the solid-state structure of [$Os_3(CO)_{10}$(*c*-dpp)] contains a bridging or a chelating *c*-dpp ligand (Scheme 1).

In conclusion, ^{31}P NMR is a good diagnostic tool for predicting whether the coordination mode of phosphorus bidentate ligands in trimetallic cluster compounds is chelating or bridging. The structures containing the ligands in either coordination mode in [$M_3(CO)_{10}(\mu_2$-η^2-(L–L))] or [$M_3(CO)_{10}(\mu_1$-η^2-(L–L))] such as observed in **1**, **3** [4], or **5** [5], may have comparable stability and can interconvert to each other in solution at high temperatures. The subsequent coordination of the olefinic moiety of the chelating *c*-dpp or dma then makes feasible the conversion from [$M_3(CO)_{12}$] to **2**, **4**, and **6**, respectively [3–5] (Scheme 1).

Acknowledgment

We wish to thank the National Science Council of the Republic of China for the financial support of this research (Contract No. NSC82-0208-M006-32).

References

1 K.-B. Shiu, C.-C. Chou, S.-L. Wang and S.-C. Wei, *Organometallics, 9* (1990) 286, 2632.
2 W.R. Cullen, P.S. Dhaliwal and C.J. Stewart, *Inorg. Chem., 6* (1967) 2256.
3 M.I. Bruce, M.L. Williams, B.W. Skelton and A.H. White, *J. Organomet. Chem., 306* (1986) 115.
4 (a) W.R. Cullen and D.A. Harbourne, *Inorg. Chem., 9* (1970) 1839; (b) P.J. Roberts and J. Trotter, *J. Chem. Soc. A*, (1970) 3246. (c) (1971) 1479.
5 (a) F.W.B. Einstein and J. Trotter, *J. Chem. Soc. A*, (1967) 824; (b) W.R. Cullen, D.A. Harbourne, B.V. Liengme and J.R. Sams, *J. Am. Chem. Soc., 90* (1968) 3293; (c) *Inorg. Chem., 8* (1969) 95; (d) *Inorg. Chem., 8* (1969) 1464; (e) F.W.B. Einstein and A.-M. Svensson, *J. Am. Chem. Soc., 91* (1969) 3663; (f) W.R. Cullen, D.A. Harbourne, B.V. Liengme and J.R. Sams, *Inorg. Chem., 9* (1970) 702; (g) P.J. Robbetts and J. Trotter, *Inorg. Chem., 9* (1970) 2137.
6 (a) M.I. Bruce, G. Shaw and F.G.A. Stone, *J. Chem. Soc., Dalton Trans.*, (1972) 2094; (b) M.I. Bruce, T.W. Hambley, B.K. Nicholson and M.R. Snow, *J. Organomet. Chem., 235* (1982) 83.
7 G.A. Foulds, B.F.G. Johnson and J. Lewis, *J. Organomet. Chem., 294* (1985) 123.
8 (a) T. Venalainen, J. Pursiainen and T.A. Pakkanen, J. Chem. Soc., Chem. Commun., (1985) 1348; (b) M.I. Bruce, M.G. Humphrey, M.R. Snow, E.R.T. Tiekink and R.C. Wallis, *J. Organomet. Chem., 314* (1986) 311.
9 (a) J. Evans, B.P. Gracey, L.R. Gray and M. Webster, *J. Organomet. Chem., 240* (1982) C61; (b) A.J. Deeming, S. Donovan-Mtunzi and S.E. Kabir, *J. Organomet. Chem., 333* (1987) 253; (c) E. Sappa, G. Predieri, A. Tiripicchio and C. Vignali, *J. Organomet. Chem., 378* (1989) 109.
10 G. Suss-Fink and H. Jungbluth, *J. Organomet. Chem., 352* (1988) 185.
11 (a) J.R. Shapley, S.I. Richter, M.R. Churchill and R.A. Lashewycz, *J. Am. Chem. Soc., 99* (1977) 7384; (b) M.R. Churchill and R.A. Lashewycz, *Inorg. Chem., 17* (1978) 1950; (c) M.R. Churchill, R.A. Lashewycz, J.R. Shapley and S.I. Richter, *Inorg. Chem., 19* (1980) 1277.
12 V.G. Albano, D. Braga, R. Ros and A. Scrivanti, *J. Chem. Soc., Chem. Commun.*, (1985) 866.
13 S.O. Grim, W.L. Briggs, R.C. Barth, C.A. Tolman and J.P. Jesson, *Inorg. Chem., 13* (1974) 1095.
14 K.-B. Shiu, C.-J. Chang, Y. Wang and M.-J. Cheng, *J. Chin. Chem. Soc. (Taipei), 36* (1989) 25.
15 (a) F.A. Cotton and B.E. Hanson, *Inorg. Chem., 16* (1977) 3369; (b) A.W. Coleman, D.F. Jones, P.H. Dixneuf, C. Brisson, J.-J. Bonnet and G. Lavigne, *Inorg. Chem., 23* (1984) 952.
16 M.R. Churchill, F.J. Hollander and J.P. Hutchinson, *Inorg. Chem., 16* (1977) 2655.
17 E.J. Forbes, N. Goodhand, D.L. Jones and T.A. Hamor, *J. Organomet. Chem., 182* (1979) 143.
18 D.A. Brandes and R.J. Puddephatt, *Inorg. Chim. Acta, 113* (1986) 17.
19 G. Lavigne, N. Lugan and J.J. Bonnet, *Acta Cryst. B, 38* (1982) 1911.
20 R.E. Benfield, B.F.G. Johnson, P.R. Raithby and G.M. Sheldrick, *Acta Cryst. B, 34* (1978) 666.
21 J.J. Rafalko, P.M. Watson, D.H. Malueg, R.E. Davis and B.C. Gates, *Inorg. Chem., 20* (1981) 3540.
22 B.F.G. Johnson (Ed.), *Transition Metal Clusters*, Wiley, New York, 1980, Chapter 5.